Preparation of Core–Shell Nanoparticle-Based Hindered Amine Stabilizer and Its Application in Polyoxymethylene

Bin You, Daojun Zhou, Shiling Zhang, Fan Yang, Xiancheng Ren

College of Polymer Science and Engineering, Sichuan University, Chengdu 610065, China

Received 3 December 2011; accepted 31 January 2012
DOI 10.1002/app.36923
Published online in Wiley Online Library (wileyonlinelibrary.com).

ABSTRACT: Core–shell nanoparticles chemically functionalized by hindered amine stabilizer (HAS), poly(BA-MMA-*co*-PMPA) (PBMP), were prepared by two-stage emulsion polymerization from butyl acrylate, methyl methacrylate, and 1,2,2,6,6-pentamethylpiperidin-4-yl acrylate. The incorporation of HAS into the particles was confirmed by nuclear magnetic resonance (^{1}H-NMR) and the core–shell microstructure of PBMP particles was revealed by transmission electron microscopy. Furthermore, PBMP capable of one-step toughening and photostabilizing, was melt-blended with polyoxymethylene (POM), and its dispersion in POM was investigated by scanning electron microscope. The results showed that the core–shell nanoparticles could be well dispersed in POM matrix, indicating its good compatibility with POM. The UV resistance and impact resistance of POM were obviously improved by the HAS-functional core–shell nanoparticles simultaneously. In addition, the core–shell nanoparticles could confer excellent protection to the surface of POM from UV-light damage, regardless of the adverse effects on the thermal-oxidative stability of POM, as investigated by thermogravimetry analysis under aerobic condition. © 2012 Wiley Periodicals, Inc. J Appl Polym Sci 000: 000–000, 2012

Key words: UV aging; toughness; polyoxymethylene; hindered amine stabilizer

INTRODUCTION

Polyoxymethylene (POM), one of the major engineering thermoplastics, has a wide range of applications in industry due to its high mechanical strength, excellent abrasion resistance, fatigue resistance, dimensional stability, corrosion resistance, and moldability, for example, in electrical and electronic applications, automotive applications, and precision machine applications.[1–9] However, low UV resistance, low impact toughness, poor thermal stability, and sensitivity to notch limit its range of applications. Pure POM exposed to high-energy UV radiation undergoes radiation-induced chain scission, resulting in the discoloration, cracking of surface, stiffening, and decrease in the mechanical properties, which shortens their service life as a consequence of photo-oxidation.[10–13] Therefore, its UV resistance becomes an important consideration.

Generally, as the main way to solve the problem of photostabilization of POM, addition of UV stabilizers has been successfully used to prevent POM from UV ageing, such as UV shield agents, UV absorbers, and hindered amine stabilizers (HAS). However, UV shield agents including carbon black, titanium oxide, and zinc oxide have negative effects on the color of polymeric materials, and so do the UV absorbers, such as benzophenone derivatives, benzotriazole derivatives, and triazine derivatives. Nevertheless, HAS have no adverse influence on the color of polymers. Most important of all, HAS are very effective photostabilizers, called free radical scavenger, which can protect polymers by a multifunctional mechanism including free radicals scavenging, deactivation of peroxidic species and quenching of singlet oxygen.[14–17] In addition, stabilizers must be effective over long periods of time. It is important that they do not volatilize, be leached out or otherwise be removed from plastic materials. However, low-molecular weight UV stabilizers would easily lose photostabilization in long-term use, because of its easy migration and poor extraction resistance. The problem caused by low molecular weight stabilizers can be overcome through the use of reactive UV stabilizers and high molecular weight UV stabilizers.[18–22]

The toughing of POM by blending with elastomers is commonly proposed, for example, by polyurethane elastomer and polyacrylate elastomer.[23–25] Therefore, it is of interest to study one-step photostabilizing and toughing of POM with impact modifiers functionalized by UV stabilizers.

In this study, core–shell nanoparticles containing HAS, PBMP, which were capable of one-step toughening and photostabilizing, were prepared through

Correspondence to: X. Ren (xiancren@sina.com).
Contract grant sponsor: National Natural Sciences Foundation of China; contract grant number: 50873069.

two-stage emulsion polymerization, and the influence on the impact resistance, UV resistance, and thermal-oxidative stability of POM were investigated. The results showed that the addition of PBMP nanoparticles could increase the toughness and photostabilization of POM but had an adverse effect on the thermal-oxidative stability of POM.

EXPERIMENTAL

Materials

Methyl methacrylate (MMA, analytical reagent) and butyl acrylate (BA, analytical reagent) were provided by Tianjin Bodi Chemical of China (Tianjin, China), were distilled before application. 1,2,2,6,6-Pentamethyl-4-piperidinol (PMP, purity > 98.0%) was provided by Jinchun Meibang Chemical (Wuhan, China). 1,2,2,6,6-Pentamethylpiperidin-4-yl acrylate (PMPA) was prepared according to previous study.[19] Analytical reagent grade sodium dodecyl sulfate (SDS), potassium persulfate (KPS), tetrahydrofuran (THF), calcium chloride ($CaCl_2$), sodium bicarbonate ($NaHCO_3$), and divinyl benzene (DVB) were provided by Kelong Chemical Reagent Factory of China (Chengdu, China). POM used in this study, was a commercial grade copolymer and supplied by Yuntianhua (M90, Yunnan, China) with a melt flow index of 9.0 g/10 min.

Preparation of core–shell nanoparticles

Poly(BA-MMA-*co*-PMPA) (PBMP) and poly(BA-MMA) (PBM) were synthesized by a conventional semibatch two-stage emulsion polymerization process. The detailed procedure is described as follows: mixtures of the core and shell substances listed in Table I were vigorously stirred in 250-mL three-necked flasks for 1 h at room temperature to prepare core and shell monomer pre-emulsion, respectively. Then, one-fourth of the core pre-emulsion and 0.2 g KPS were added to a 500-mL four-necked flask under moderate stirring. The reaction temperature was increased to 80°C. After additional 0.5 h, the remaining three-fourth of core pre-emulsion was dropped into the flask within 2 h. After completion of feeding, the reaction was carried out for 1 h at 80°C to prepare core emulsion. Afterwards, shell pre-emulsion was added dropwise to the resulting core emulsion within 2 h. After adding the shell pre-emulsion, the reaction was carried out for additional 2 h at 90°C. The emulsion was coagulated with 5% $CaCl_2$ aqueous solution, filtered, and washed with 80°C-deionized water to demulsify. At last, the particles were dried in vacuum drying oven at 85°C for 72 h.

TABLE I
Recipes for Core–Shell Nanoparticles Preparation

	PBMP		PBM	
Components	Core (g)	Shell (g)	Core (g)	Shell (g)
BA	80.0	–	80	–
MMA	–	28.0	–	40
PMPA	–	12.0	–	–
DVB	1.2	–	1.2	–
KPS	0.20	0.15	0.20	0.15
SDS	1.6	0.8	1.6	0.8
$NaHCO_3$	0.5	–	0.5	–
DI water	120	60	120	60

Sample preparation

POM/PBMP (10 wt % PBMP) and POM/PBM/PMP blends (10 wt % PBM, 1.0 wt % PMP) were prepared through melt-blend process by a HT-30 corotating twin-screw extruder (Nanjing Rubber and Plastics Machinery Plant, China). The blending temperature was 185°C. The samples for UV irradiation and mechanical properties testing were prepared via injection molding by a LS-26 injection molding machine (Nissei Plastic Industrial, Japan) operating at 190°C. The specimens were kept at 23°C for 24 h before testing.

UV-aging test

Accelerated UV-aging tests were carried out at 35 ± 2°C with air circulating with a weathering tester equipped with two 500-W Ga–In source lamp with a maximum intensity at 365 nm. The intensity of irradiation was 3.0 W/m^2, measured by a UV-A UV irradiance meter (Photoelectric Instrument Factory of Beijing Normal University, China). Samples for testing were taken at a series of intervals (0, 200, 400, 600, and 800 h). The size of samples for UV-aging test is 150 × 40 × 10 mm^3.

Measurements and characterization

Nuclear magnetic resonance (^{1}H-NMR)

^{1}H-NMR spectrum was recorded on a Varian INOVA-400 spectrometer (Varian Company), the emission frequency was 400 MHz, and the scanning range was 0–15 of 400 MHZ. The samples were purified by precipitation of chloroform solution into methanol. Deuterated chloroform and tetramethylsilane were used as solvent and internal standard, respectively.

Transmission electron microscope

Transmission electron microscopy (TEM) micrograph of the core–shell polyacrylate modifier was taken with a Hitachi H-600 TEM (Hitachi Company, Japan) at an accelerating voltage of 100 kV. The sample was diluted with deionized water and stained with 3% phosphotungstic acid solution before measurement.

Scanning electron microscope

The dispersion of PBMP modifier in POM matrix was examined by a Hitachi X650 scanning electron microscopy (SEM; Hitachi Company, Japan). The fracture surface was obtained by breaking the molded bar at liquid nitrogen temperature (−196°C) and etching by THF for 48 h at room temperature to eliminate the modifier. The sample was coated with a thin film of gold before measurement.

Weight loss measurement

The weight of the samples before and after UV irradiation was measured on a balance. The percent weight loss was calculated as follows:

$$\text{weightlosss}\ (\%) = \frac{m_0 - m_n}{m_0} \times 100\% \qquad (1)$$

where m_0 is the weight of the sample without irradiation, m_n is the weight of the sample after n-h UV irradiation.

Notched impact strength

The notched Izod impact strength was tested on a UJ-40 tester (Chengde Testing Machine Factory, China), according to ISO 180: 2000.

Irradiated surface analysis

The UV-irradiated surfaces of the molded bars were studied by a UM 200i reflected metallurgical microscope (Chongqing UOP Photoelectric Technology, China). The magnifying power is 100.

Thermogravimetric analysis

Thermogravimetric analysis (TGA) was performed with a TG 209F1 Iris (NETZSCH Company, Germany). Samples of about 10 mg were heated in air atmosphere with a purge gas stream of 60 mL/min in aluminum pans at a heating rate of 10°C/min from 50 to 800°C. The onset temperature (i.e., the degradation start temperature) was defined at a mass loss of 3% of the initial sample mass because of the irreproducibility of the temperatures determined by the tangent method.[12]

RESULTS AND DISCUSSION

^{1}H-NMR analysis of PBMP

The ^{1}H-NMR spectra for monomer PMPA, PBMP, and PBM are demonstrated in Figure 1. From the ^{1}H-NMR spectrum for PMPA, the chemical shifts around 1.0 and 1.1 assigned to —CH_3 protons, the chemical shift around 1.6 and 1.8 ppm associated with —CH_2— protons, the chemical shifts around 2.2 and 5.1 ppm attributed to —N—CH_3 and —O—CH protons, respectively, and the chemical shifts around 5.8, 6.1, and 6.4 ppm originating from CH_2=CH— are observed, which is consistent with Reference 19.

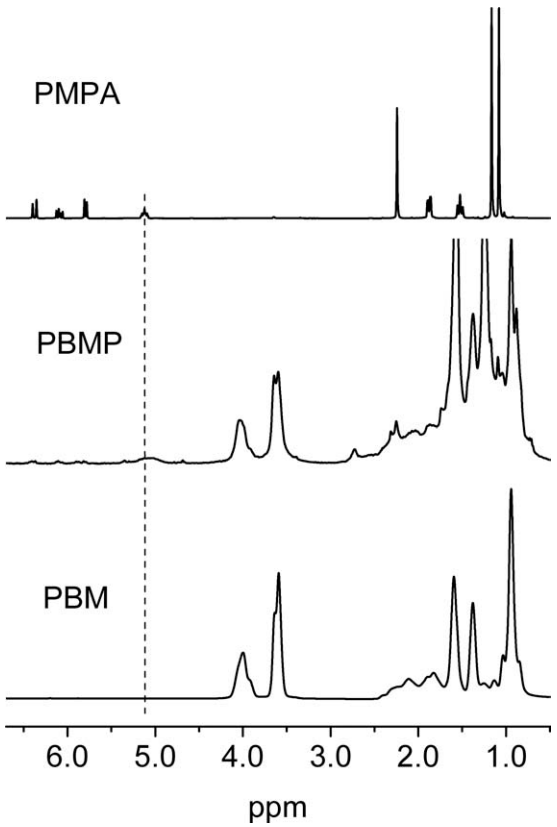

Figure 1 ^{1}H-NMR spectra of PBMP, PBM, and PMPA.

The chemical shifts around 0.9 and 4.0 ppm assigned to —CH_3 and —O—CH_3 protons in the side chains of PBA, respectively, the chemical shifts around 1.4 and 1.6 ppm associated with —CH_2— protons in the side chains of PBA and the chemical shifts around 1.8 and 2.2 ppm originating from —CH_2— and —CH— protons in the main chains of PBA are observed for both PBM and PBMP.[26] The chemical shifts around 1.2, 1.6, and 3.6 ppm attributed to —CH_3, —CH_2—, and —O—CH_3 protons, respectively, in PMMA are also observed in ^{1}H-NMR spectra for both PBMP and PBM.[26] However, the chemical shifts of —CH_3, —CH_2—, and —N—CH_3 protons in PMPA overlap with the similar structures from PBA and PMMA, except for —O—CH protons. Therefore, it could be seen from Figure 1 that a wide weak peak around 5.1 ppm observed for PBMP is the characteristic chemical shift of —O—CH proton in PMPA as shown in the spectrum for the monomer. As discussed above, it can be concluded that HAS has been successfully incorporated into the PBMP particles.

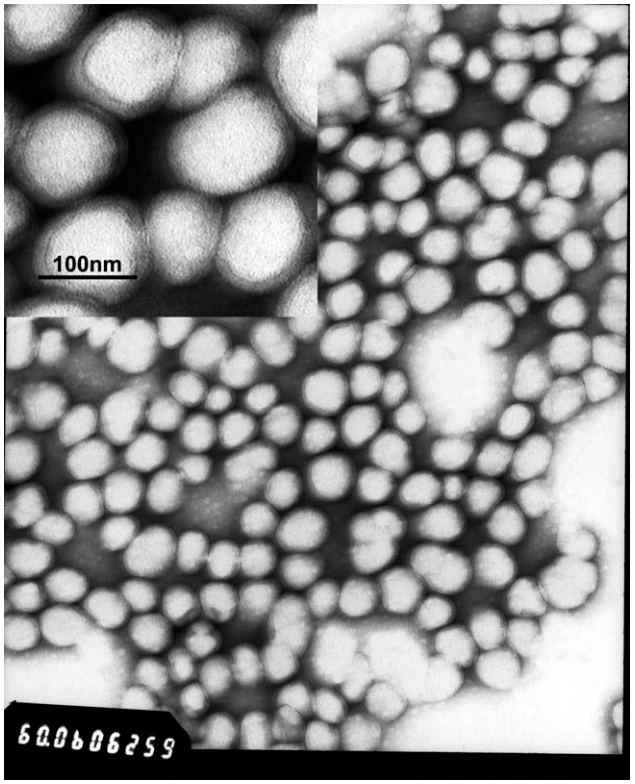

Figure 2 TEM image of core–shell PBMP.

Microstructure of PBMP

The microstructure of the PBMP particles was investigated by TEM, and the image for the particles is provided in Figure 2. A core–shell structure was observed, owing to the fact that the different components of the core and shell phases have different electron penetrability, as shown in Figure 2. The white and gray regions represent crosslinked PBA core and MMA-*co*-PMPA shell, respectively, which confirms the microstructure of the HAS-functional core–shell particles. In addition, the particles have an average diameter around 100 nm. Therefore, it proves that the core–shell nanoparticles functionalized by HAS have been prepared as desired through two-stage emulsion polymerization.

Dispersion of PBMP in POM

Pure poly(butyl acrylate) (PBA) particles cannot be well dispersed in the POM matrix, due to its poor compatibility with POM and the agglomeration of PBA particles at room temperature (glass transition temperature of PBA is below room temperature). To improve the compatibility of PBA particles with POM matrix and reduce the agglomeration of PBA, it is necessary to graft polymers with high glass transition temperature and good compatibility with POM onto the surface of PBA particles to obtain a soft core and hard shell structured impact modifier. The hard shell plays two important roles: the first is to act as compatibilizing agent between PBA and POM interface; the second is to avoid the formation of coagula from pure PBA particles. Therefore, MMA monomer was chosen to graft onto the PBA core to form a hard shell, due to its good compatibility with POM and excellent UV resistance.[25] The SEM image for facture surface of the POM/PBMP blend resulting from 10-wt % PBMP addition is given in Figure 3. Two-phase morphology has been demonstrated, i.e., the dispersed phase and the continuous phase, as shown in the image. The holes with a diameter above 0.2 μm on the fracture surface are the agglomerates of the core–shell particles, and the ones with a diameter below 0.2 μm represent the core–shell particles. It could be seen from the picture that the holes are dispersed evenly in the POM matrix, indicating that PBMP nanoparticles have good compatibility with POM.

Weight loss

Polymeric materials damaged by UV light will release small molecules, such as hydrogen gas, carbon dioxide, carbon monoxide, water, etc., and the mass will run down accordingly.[20] Therefore, to determine the degree of UV degradation, the weight loss of the testing samples was investigated. The results presented in Figure 4 show that all the samples exhibit weight loss in varying degrees after UV irradiation, however, POM/PBMP has less weight loss in comparison to pure POM and POM/PBM/PMP and the degree of weight loss is POM > POM/PBM/PMP > POM/PBMP. It is attributed to the fact that POM can be UV-stabilized by HAS. However, on the one hand, the UV-stabilizing effect of low

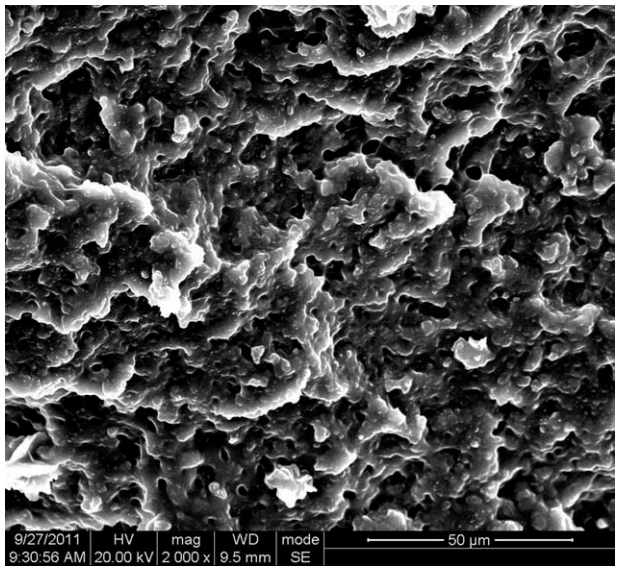

Figure 3 SEM image for POM/PBMP blend.

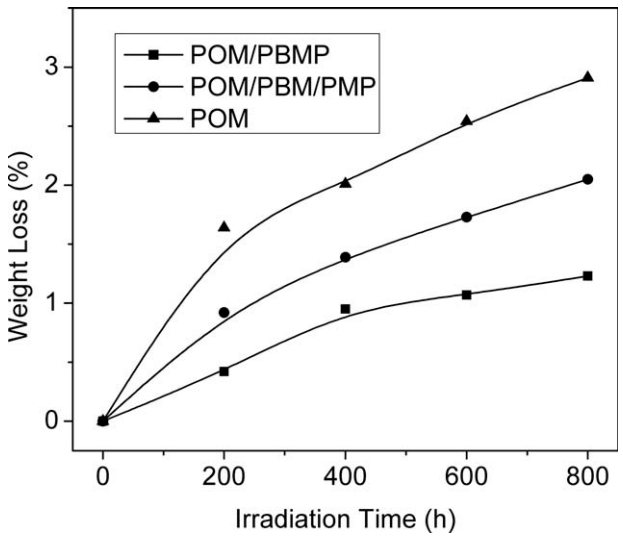

Figure 4 Weight loss for POM, POM/PBMP, and POM/PBM/PMP after UV irradiation.

molecular weight UV-stabilizer PMP was seriously deteriorated as it could be easily removed from POM matrix during UV irradiation. On the other hand, the PBMP particles chemically bound HAS have better resistance to migration and extraction and could impart outstanding protection to POM from UV irradiation. Therefore, POM/PBMP shows better UV resistance compared with POM/PBM/PMP.

Impact properties analysis

POM, with poor notched impact resistance, is mainly toughened by blending with polyurethane elastomer and polyacrylate elastomer. However, polyacrylate has better UV resistance, as polyurethane would easily turn yellow after UV irradiation.[23–25] Pure POM irradiated by UV light undergoes a series of photo-oxidative degradation, resulting in deterioration of mechanical properties, especially, the notched impact strength. PBMP nanoparticles are a soft core and hard shell structured impact modifier functionalized by HAS, which can be used as UV stabilizer to stabilize POM. In addition, HAS incorporated into modifier could be effective over a long time, because the stabilizer would not be easily lost during processing at high temperature and outdoor applications. The notched Izod impact strength for pure POM, POM/PBMP, and POM/PBM/PMP before and after UV irradiation is shown in Figure 5.

The notched impact strength of POM was increased by about 36 and 40%, respectively, with 10 wt % addition of PBMP and PBM (in Fig. 5). However, the latter provided extra 4% improvement in the notched impact strength for POM. One possible explanation is that PMMA homopolymer has better compatibility with POM than MMA-*co*-PMPA copolymer. It could be attributed to the fact that the solubility parameter for PMMA (δ_{PMMA} is about 9.5 $cal^{0.5}/cm^{1.5}$) is slightly closer to POM (δ_{POM} is about 11.1 $cal^{0.5}/cm^{1.5}$) than MMA-*co*-PMPA ($\delta_{MMA\text{-}co\text{-}PMPA}$ is about 9.1 $cal^{0.5}/cm^{1.5}$ estimated according to Ref. 27).

The findings according to Figure 5 show that both POM/PBMP and POM/PBM/PMP blends exhibit higher percentage retention of impact strength in comparison to pure POM, indicating that PBMP and PBM/PMP systems confer good protection to POM from UV damage. It is noted that POM/PBMP demonstrates higher percentage retention of notched impact strength than POM/PBM/PMP, especially after 400-h UV irradiation. The reason is that the low molecular weight UV-stabilizer PMP was gradually lost as the irradiation time increased, which greatly deteriorated the photostabilizing effect of POM/PBM/PMP. Moreover, the percentage retention of notched impact strength for POM/PBMP after 800-h UV irradiation is about 10% higher than that for POM/PBM/PMP. Therefore, PBMP nanoparticles can provide toughening and long-term photostabilization to POM simultaneously.

Surface morphology analysis

Figure 6 presents the pictures of the surfaces for POM, POM/PBMP, and POM/PBM/PMP after 200, 400, 600, and 800 h UV irradiation. It is noted that the size of the surface crazing for pure POM after UV irradiation is about 20 μm; however, the size of the surface crazing for both POM/PBMP and POM/PBM/PMP is less than 10 μm. The size of the surface crazing for pure POM after 400-h UV irradiation increased sharply compared with that after 200-h

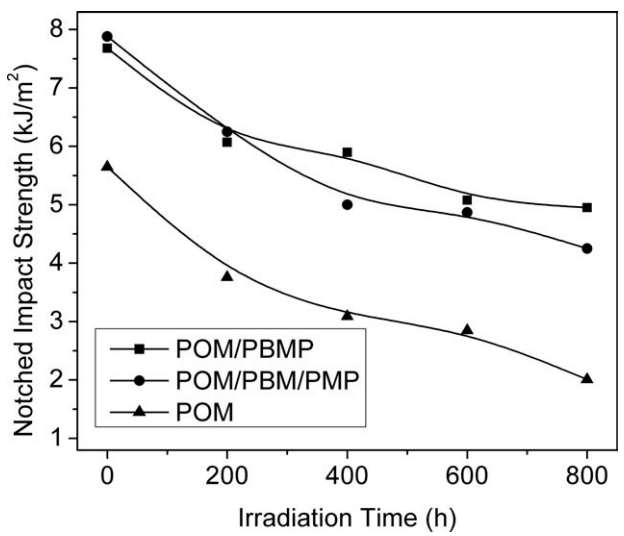

Figure 5 Notched impact strength for POM, POM/PBMP, and POM/PBM/PMP after UV irradiation.

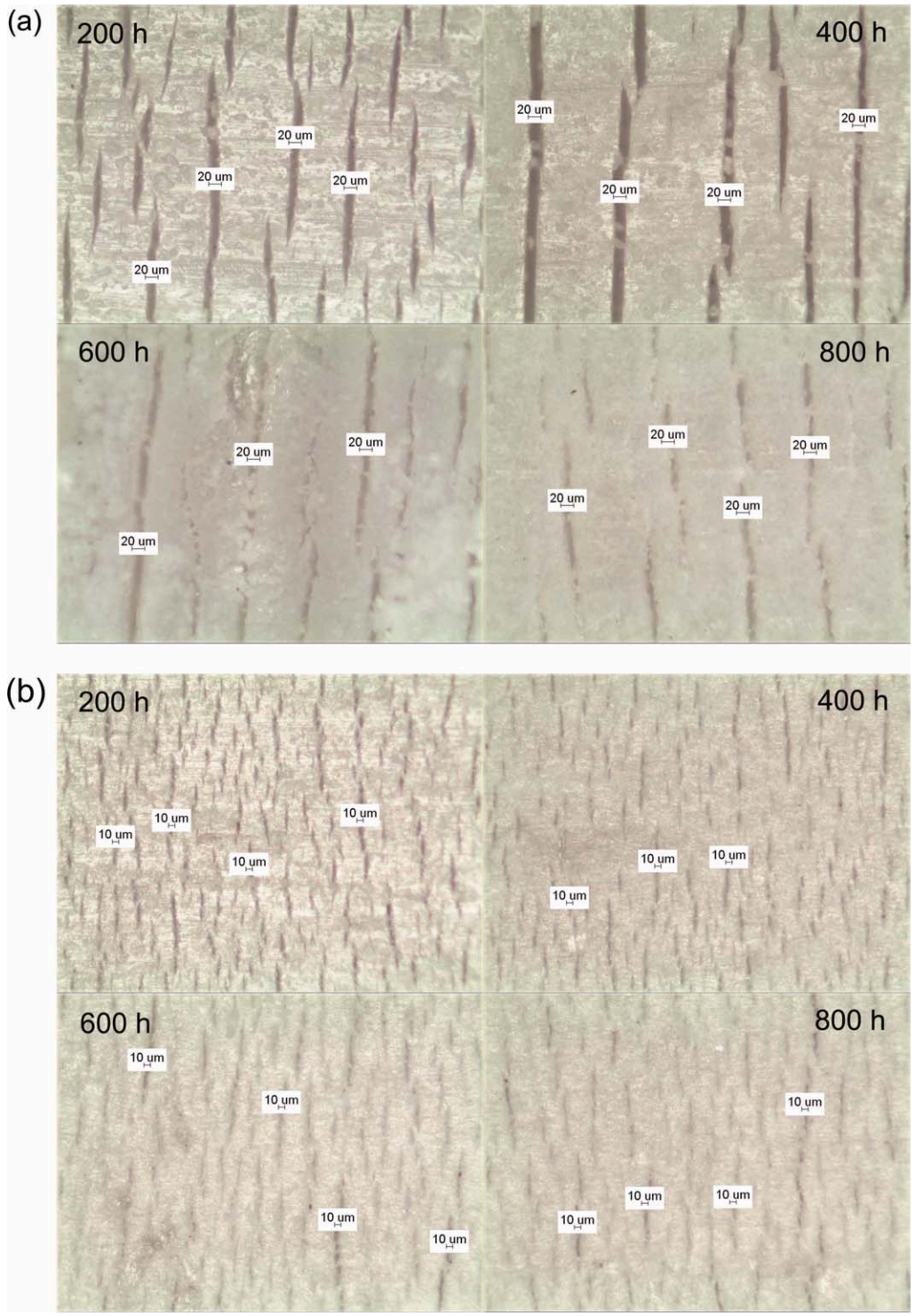

Figure 6 Pictures of the surfaces for (a) POM, (b) POM/PBMP, and (c) POM/PBM/PMP after UV irradiation. [Color figure can be viewed in the online issue, which is available at wileyonlinelibrary.com.]

UV irradiation. However after 400-h UV irradiation, the size of the surface crazing hardly increased. Nevertheless, the size of surface crazing for both POM/PBMP and POM/PBM/PMP did not increase obviously with the increase of UV-irradiation time. Moreover, pure POM after 600-h UV irradiation presents a white powder on the surface, a phenomenon called "chalking."[25] However, the same phenomenon has not been found for both POM/PBMP and POM/PBM/PMP. It is attributed to two factors: the first one is that PBMP and PMP can protect the surface from UV damage; the second one is that the extension of the surface crazing can be retarded by the core–shell nanoparticles. Additionally, the

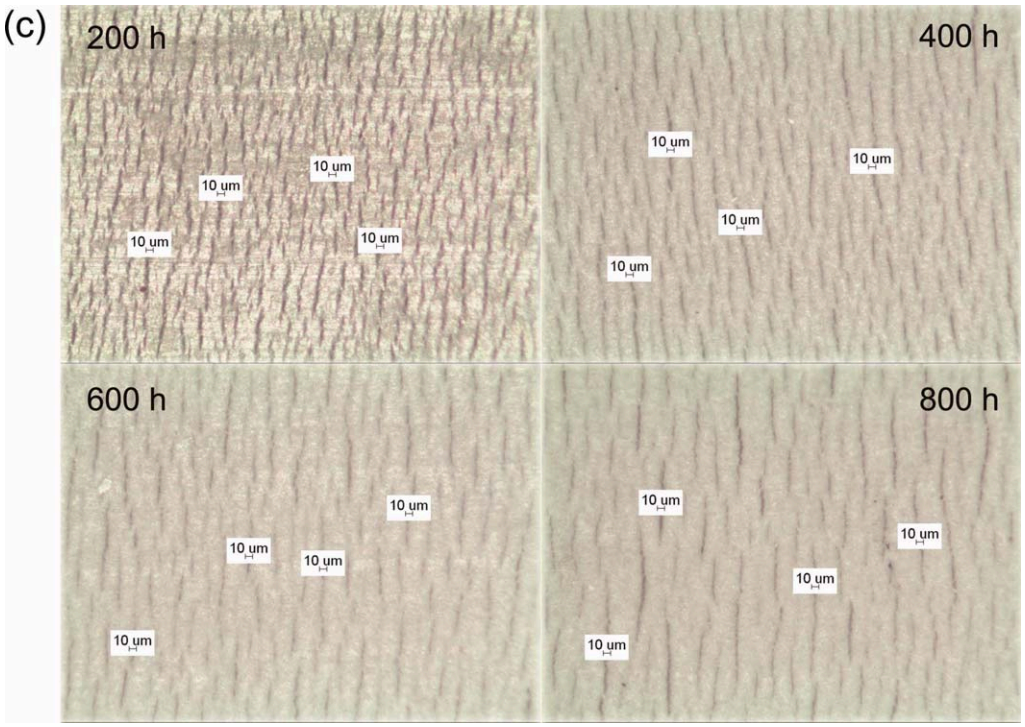

Figure 6 (Continued)

intensity of the surface crazing for POM/PBMP are inferior to POM/PBM/PMP, indicating that PBMP provides better protection to the surface of POM from UV damage, because of the loss of low molecular weight UV-stabilizer PMP during the processing and UV irradiation. It can be concluded that both PBMP and PBM/PMP could impart good protection to POM from UV damage. More important, PBMP could confer more significant photostabilization to the surface of POM testing bars than PBM/PMP system.

Thermal-oxidative stability analysis

The thermal-oxidative stability of PBMP was studied by thermogravimetric analysis (TGA) in air atmosphere, attributed to the fact that the nanoparticles have to be blended with POM above 180°C under aerobic condition. Its effect on POM before and after UV irradiation was investigated as well to determine the degree of UV degradation. The results are presented in Table II and Figures 7–9.

TABLE II
Thermal-Oxidative Decomposition Temperatures for PBMP, PBM, POM, POM/PBMP, and POM/PBM/PMP

Samples	T_{onset} (°C)	T_{50} (°C)	T_{max} (°C)	T_{end} (°C)
PBMP	294	365	367	505
PBM	270	335	282	504
POM	278	305	307	346
POM/PBMP	222	279	278	377
POM/PBM/PMP	212	276	275	376
Irradiated POM	153	283	295	345
Irradiated POM/PBMP	210	261	254	372
Irradiated POM/PBM/PMP	205	259	250	371

It could be seen from Figure 7 that both PBMP and PBM exhibit a three-step thermal-oxidative degradation pattern. The first degradation stage, caused by the degradation of PMMA segments involving unzipping of the chain starting at both the vinylidene end groups and the weaker head-to-head linkages,[28–30] appears from the onset decomposition

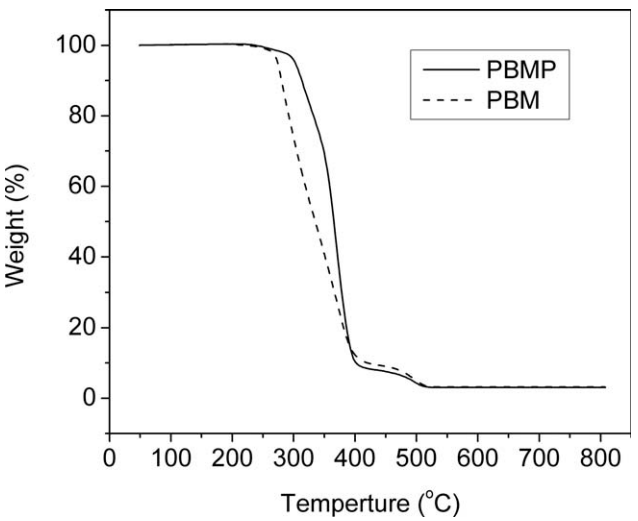

Figure 7 TGA curves for PBMP and PBM under air.

temperatures (T_{onset}) to 330°C. The second decomposition stage starts from 330°C and ends around 450°C, attributed to the random scission of the polymer chains.[28,31,32] The final stage, which occurs at temperatures above 450°C, concerns a minor part of residue which is associated with the formation of primary char and therefore decompose at lower rate.[33] As shown in Table II, the onset decomposition temperature (T_{onset}) and 50% weight loss temperature (T_{50}) for PBMP are increased by 24 and 30°C, respectively, in comparison to PBM. It is noteworthy, however, that PBMP provides a 85°C improvement in the temperature at maximum weight loss rate (T_{max}). Therefore, PBMP exhibits better thermal-oxidative stability than PBM, attributed to the reduction of the relative abundance of vinylidene end groups and the weaker head-to-head linkages in PMMA segments by copolymerization of PMPA with MMA, the scavenging of radical species and deactivation of peroxide by HAS.[28–30,34,35]

In the presence of oxygen, pure POM undergoes one-step thermal-oxidative decomposition from about 278 to 346°C, which is consistent with previous observation,[13] as shown in Figure 8. However, both POM/PBM/PMP and POM/PBM show a two-stage degradation pattern (in Fig. 8). The first stage, between the onset decomposition temperature and 310°C, is mainly attributed to the formation of peroxide from PMMA segments under aerobic condition,[36] which initiates the depolymerization of POM.[37] The second stage appears from 310°C to the end of decomposition, due to the random chain scission of PBA, MMA-*co*-PMPA and residual portion of POM. Therefore, the thermal-oxidative stability of both POM/PBM/PMP and POM/PBM is inferior to pure POM. However, the onset decomposition temperature for POM/PBM is about 10°C higher than

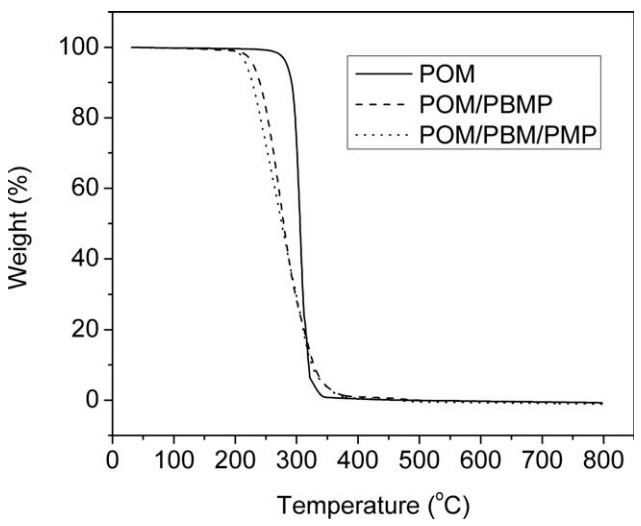

Figure 8 TGA curves for POM, POM/PBMP and POM/PBM/PMP before UV irradiation under air.

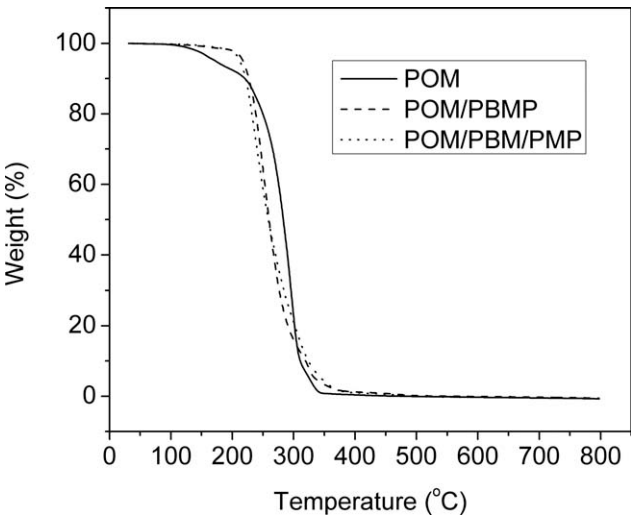

Figure 9 TGA curves for POM, POM/PBMP and POM/PBM/PMP after UV irradiation under air.

POM/PBM/PMP. One explanation is that the peroxide could be deactivated by HAS from PBMP, which retards the decomposition of POM/PBMP; however, the loss of PMP during processing and high temperature has an detrimental effect on the deactivation of peroxide, leading to the decrease of onset decomposition temperature of POM/PBM/PMP.

The TGA curves for POM/PBMP and POM/PBM/PMP after 800-h UV irradiation are similar with those before UV irradiation, except for a decrease in corresponding temperatures, indicating that no change occur in the degradation pattern after UV irradiation, as shown in Figure 9. However, a significant difference between the TGA curves for POM before and after UV irradiation observed is that a new degradation stage appears from 153°C and ends around 230°C, owing to the degradation of chalked layer on the irradiated surface of POM testing bars. In this stage, the decomposition rate is about 8%, indicating that the photodegradation occurs most up of the irradiated surface. However, the onset decomposition temperatures for POM/PBMP and POM/PBM/PMP after UV irradiation decrease slightly, due to the excellent protection from UV damage by PBMP and PMP, respectively.

CONCLUSIONS

The core–shell nanoparticles bound with HAS, PBMP, were successfully prepared by emulsion polymerization and showed better thermal-oxidative stability than PBM. Furthermore, the core–shell nanoparticles had good compatibility with POM and could be well dispersed in the matrix. Although the addition of the particles had a detrimental effect on the thermal-oxidative stability of POM, the onset decomposition temperature for POM/PBMP blend

before UV irradiation was above 220°C, which was beyond the processing temperature of POM (the processing temperature is 170–195°C). Most important of all, the toughness and photostabilization of pure POM were enhanced by PBMP core–shell nanoparticles simultaneously. In addition, PBMP can impart better photostabilization to POM than low molecular weight UV-stabilizer PMP.

References

1. Hasegawa, S.; Takeshita, H.; Yoshii, F.; Sasaki, T.; Makuuchi, K.; Nishimoto, S. Polymer 2000, 41, 111.
2. Zhao, X. W.; Ye, L. J Polym Sci Part B: Polym Phys 2010, 48, 905.
3. Hu, Y. L.; Ye, L.; Zhao, X. W. Polymer 2006, 47, 2649.
4. Hama, H.; Tashiro, K. Polymer 2003, 44, 6973.
5. Thontree, K.; Yasushi, K.; Toshikazu, U.; Daigo, N.; Wandee, T.; Yupin, P.; Suwabun, C. Polymer 2008, 49, 1676.
6. Shi, J.; Jing, B.; Zou, X. X.; Luo, H. J.; Dai, W. L. J Mater Sci 2009, 44, 1251.
7. Luftl, S.; Archodoulak, V. M.; Glantschnig, M.; Seidler, S. J Mater Sci 2007, 42, 1351.
8. Yu, N.; He, L. H.; Ren, Y. Y.; Xu, Q. Polymer 2011, 52, 472.
9. Duan, Y. F.; Li, H. L.; Ye, L.; Liu, X. L. J Appl Polym Sci 2006, 99, 3085.
10. Sirirat, W.; Supakanok, T.; Akaraphol, P.; Chaturong, E. Polym Test 2008, 27, 971.
11. Cottin, H.; Gazeau, M. C.; Doussin, J. F.; Raulin, F. J. Photochem Photobiol A: Chem 2000, 135, 53.
12. Luftl, S.; Archodoulaki, V. M.; Seidler, S. Polym Degrad Stab 2006, 91, 464.
13. Archodoulaki, V. M.; Luftl, S.; Seidler, S. Polym Degrad Stab 2004, 86, 75.
14. Sun, G. J.; Jang, H. J.; Kaang, S. Y.; Chae, K. H. Polymer 2002, 43, 5855.
15. Mosnacek, J.; Chmela, S.; Theumer, G.; Habicher, W. D.; Hrdlovic, P. Polym Degrad Stab 2003, 80, 113.
16. Malik, J.; Ligner, G.; Avirr, L. Polym Degrad Stab 1998, 60, 205.
17. Kikkawa, K. Polym Degrad Stab 1995, 49, 135.
18. Bojinov, V. B.; Grabchev, I. Polym Degrad Stab 2001, 74, 543.
19. Chmela, S.; Lajoie, P.; Hrdlovic, P.; Lacoste, J. Polym Degrad Stab 2001, 71, 71.
20. Zhao, Y.; Dan, Y. Eur Polym J 2007, 43, 4541.
21. Konstantinova, T.; Konstantinovb, H.; Avramov, L. Polym Degrad Stab 1999, 64, 235.
22. Wilen, C. E.; Auer, M.; Stranden, J.; Nasman, J. H. Macromolecules 2000, 33, 5011.
23. Cheng, Z. G.; Wang, Q. Polym Int 2006, 55, 1075.
24. Gao, X. L.; Qu, C.; Fu, Q. Polym Int 2004, 53, 1666.
25. Ren, X. C.; Chen, L.; Zhao, H. J.; Dan, Y.; Cai, X. F. J Macromol Sci Part B: Phys 2007, 46, 411.
26. Kanmuri, S.; Moholkar, V. S. Polymer 2010, 51, 3249.
27. He, M. J.; Chen, W. X.; Dong, X. X. Polymer Physics, 1st ed.; Fudan University Press: Shanghai, 2004; Chapter 3, p 114.
28. Hirata, T.; Kashiwagi, T.; Brown, J. E. Macromolecules 1985, 18, 1410.
29. Kashiwagi, T.; Inaba, A.; Brown, J. E.; Hatada, K.; Kitayama, T.; Masuda, E. Macromolecules 1986, 19, 2160.
30. Higashi, N.; Shiba, H.; Niwa, M. Macromolecules 1989, 22, 4652.
31. Hu, Y. H.; Chena, C. Y.; Wang, C. C. Polym Degrad Stab 2004, 84, 505.
32. Zhang, F. A.; Lee, D. K.; Thomas, J. P. Polymer 2009, 50, 4768.
33. Galina, F. L.; Kun, S.; Sergei, V. L.; Camino, G.; Charles, A. W. Polym Degrad Stab 1999, 65, 395.
34. Solomon, D. H.; Swift, J. D. J App Polym Sci 1967, 11, 2567.
35. Hwang, K. J.; Kim. D. S. J Appl Polym Sci 2008, 110, 2957.
36. Kashiwagi, T.; Inaba, A.; Brown, J. E.; Hatada, K.; Kitayama, T.; Masuda, E. Macromolecules 1986, 19, 2160.
37. Nishimura, O.; Osawa, Z. Polym Photochem 1981, 1, 191.